ICAS-80-5.5

ACTIVE FLUTTER SUPPRESSION DESIGN AND TEST, A JOINT U.S.-F.R.G. PROGRAM

T. Noll*
U.S. Air Force Wright Aeronautical Laboratories
Flight Dynamics Laboratory
Wright-Patterson Air Force Base

H. Hönlinger**
Messerschmitt-Bolkow-Blohm, GmbH
Airplane Division
8012 Ottobrunn, West Germany

O. Sensburg†
Messerschmitt-Bolkow-Blohm, GmbH
Airplane Division
8012 Ottobrunn, West Germany

K. Schmidt††
Eprobungsstelle 61 der Bundeswehr
BWB-AFB-LG IV 9
Flugplatz
8072 Manching, West Germany

Abstract

A wing/store active flutter suppression system was designed, fabricated and installed on the F-4F aircraft to demonstrate and evaluate the concept in flight. The design used the existing autopilot and trailing edge ailerons with improved high-gain actuators. The feedback system used outboard wing accelerometers combined in a manner defined by optimal control theory. The external stores were internally modified and were used as a flutter stopper for flight safety during the tests. Identification problems attributed to structural nonlinearities in the wing pylon-store system were encountered during the ground and flight tests. As a result, high speed flights with the active flutter suppression system operating have not yet been accomplished. To describe the tests completed, open loop diagrams as well as damping curves for important elastic modes are presented. In addition, recent results of an active flutter suppression design analysis and a transonic wind tunnel test of a lightweight fighter aircraft configuration with a wing mounted external store are presented. Good correlation between the analyses and test data is shown. Based on these and other investigations, active flutter suppression is now a feasible concept. Following more extensive design and testing experience in the area of safety and adaptive control, active flutter suppression can be made operational and included in the design of future tactical aircraft.

Nomenclature

Symbols

C	wing chord
b	coefficient converting displacement to slope
F	force
g	structural damping coefficient
$\bar{g}$	acceleration due to gravity
G	actuator dynamics
h	vertical displacement
H	feedback transfer functions
M	Mach number
q	dynamic pressure
S	Laplace variable
$\bar{S}$	wing span
δ	control surface displacement
Λ	sweep angle
θ	torsion slope
ϕ	bending slope

Abbreviations

A/C	airframe
db	decibel
deg	degrees
FS	fuselage station
HL	hinge line
Hz	Hertz
Im	imaginary
in	inch
KIAS	knots indicated airspeed
Kg	kilograms
KTS	knots
LEC	leading edge control surface
M	meters
MAX	maximum
NM	Newton-meters
psf	pounds per square foot
rad	radian
RE	real
sec	second
TEC	trailing edge control surface
WS	wing station

Subscripts

F	filter
IA	inboard aft
IF	inboard forward
OA	outboard aft
OF	outboard forward
opt	optimal
TE	trailing edge

*Aerospace Engineer
**Project Manager F-4F Flutter Suppression Program
†Head of Structural Dynamics
††Manager Flight Test Center

Introduction

Wing/store flutter problems can degrade the performance of fighter-attack aircraft with a multimission, air-to-ground combat role. Flutter

speed placards or restrictions caused by the carriage of many combinations of external stores can reduce the aircraft speed capability and, as a result, decrease survivability to ground fire. Active flutter suppression has been shown to have promise of preventing or postponing store flutter, and has the potential for providing significant improvements in aircraft operational and mission effectiveness. Since active flutter suppression systems use electro-hydraulic feedback networks, the eventual integration of the system into an advanced aircraft control system is practical with a minimal increase in control hardware. During the last few years, the aerospace technical community has aggressively pursued the development of active flutter suppression technology. Recent programs completed include feasibility studies, preliminary design analyses, wind tunnel tests and flight experiments. These studies have developed the concept and data base to a stage where a full scale, flight demonstration using conventional wing control surfaces can now be undertaken.

In 1977, a much more challenging program[1] was conducted by Messerschmitt-Bolkow-Blohm (MBB) with the cooperation of the Bundesamt für Wehrtechnik und Beschaffung (BWB) and the U.S. Air Force Wright Aeronautical Laboratories (AFWAL)/Flight Dynamics Laboratory. The work was jointly sponsored by the ZTL Research program of the German Ministry of Defense and by the AFWAL. The objective of this effort was to develop and flight test an active flutter suppression system which could become a candidate for operational usage. An F-4F aircraft of the German Air Force test center in Manching (Erprobungsstelle 61 der Bundeswehr) was chosen as the test bed, since this airplane was already equipped for flight flutter tests with stores. To generate the necessary unsteady aerodynamic forces, existing control surfaces (ailerons) were used. Accelerometers located on the wing provided signals which were fed back through the existing stability augmentation system of the airplane. Preliminary results of the flight tests accomplished are presented and described in this paper.

To develop an active flutter suppression system and to resolve technical problems in actual systems implementation, the Northrop Corporation under AFWAL sponsorship designed and fabricated a 30% scale model of the YF-17 aircraft. The model had both an active leading edge and an active trailing edge control surface, and several accelerometers in the outer wing sections which could be used in any combination to produce the feedback signal. The model was first tested in 1977 with the cooperation of the NASA Langley Research Center (LaRC) in the 16-foot Transonic Dynamics Tunnel (TDT) for several control laws and different external store configurations. Flutter speed improvements of approximately 15% were successfully projected. The analytical and test results related to this test sequence are documented in an AGARD Report[2]. Beginning in 1978, the model was refurbished and modified for further active flutter suppression wind tunnel test investigations. The objective of these tests was to evaluate new control laws designed to improve the flutter speed by 30 percent or more while maintaining gain and phase margins of ±6 db and ±60°, respectively. Through USAF data exchange programs, several international organizations were invited and participated in the AFWAL sponsored wind tunnel tests. All control laws were designed at M = 0.8 for a store configuration that has a violent flutter mode. The control laws were implemented by the Northrop Corporation and tested by NASA in the 16-foot TDT in October 1979. The tested control laws provided significant flutter velocity increases[3] with acceptable gain margins; the desired phase margins, however, could not be obtained. The work performed by MBB during this program was also sponsored by the ZTL-Research Program of the German Ministry of Defense. This paper presents the analysis and test results of the MBB control law, and provides calculations to evaluate the performance of the control law at off-design flight conditions.

F-4F Flight Test Program

Selection of the Wing Mounted External Store Configuration

Previous theoretical studies on the F-4 aircraft[4] provided information about a store configuration that would flutter within the flight envelope. A store with similar mass and inertia characteristics was selected for this flight test program. A contour plot of flutter speeds for possible weight and radius of gyration combinations for this store is shown in Figure 1. The selected store mass and the corresponding radius of gyration to achieve a low flutter speed are shown in this figure. Other center-of-gravity positions which caused lower flutter speeds were excluded from consideration because of flight mechanical and load considerations.

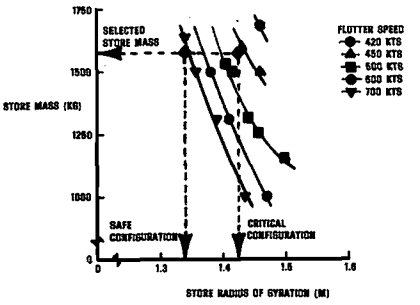

Figure 1. Flutter Speed Versus Store Mass Radius of Gyration

A flutter safe configuration was also chosen from Figure 1. This configuration could be obtained by releasing two masses inside the store thus changing only the radius of gyration. Figure 2 shows the predicted damping trends and the increase in flutter speed for the flutter-safe store configuration over the critical configuration. These configurations show about a 350 Kt increase in flutter speed or about 3% increase in structural damping at 600 Kts when the flutter-safe configuration is required. This device offers improved safety of flight during unexpected emergency conditions.

The validity of the dynamics model was established by a ground vibration test. Good correlation between test and analysis was obtained as can be seen from the comparisons of the important structural frequencies in Table 1.

Since large nonlinearities were found to exist in the pylon-store attachment, the comparisons in Table 1 are only valid for a distinct excitation level. For this store configuration, the effect of pylon pitch stiffness on the flutter speed was very pronounced. Analyses had shown that the position of the pitch node line at approximately the wing midchord gives the lowest flutter speed. The selected store configuration was designed to have this property. This modal characteristic was subsequently verified during the ground vibration tests.

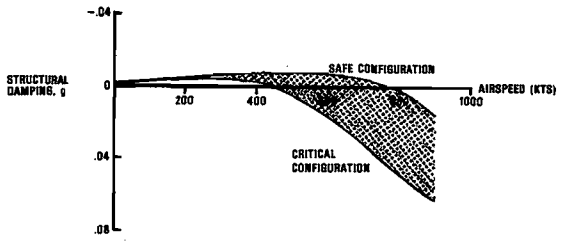

Figure 2. Calculated Flutter Speed of the Flutter-Safe Store Configuration

Table 1. Frequency Comparison of Ground Vibration Tests and Analyses

MODE	TEST (HZ)	ANALYSIS (HZ)
1ST WING BENDING	5.83	5.46
STORE YAW	5.83	5.70
STORE PITCH	6.67	6.62
STORE ROLL	8.67	8.46

Both ground vibration (Figure 3) and flight excitation tests (Figure 4) have shown that the frequencies of the critical elastic modes are amplitude-dependent. With preload and backlash in the pitch axis of the store-pylon system, various pylon pitch stiffnesses will lead to changes in the flutter speed depending on the vibration amplitudes. Because the flutter speed increases with the pylon pitch stiffness, limited amplitude flutter will be obtained. A possible explanation was defined in a study using linear approximations of the nonlinearities. The harmonic balance method was applied in this study, and nonlinear flutter calculations accomplished as discussed in the following sections.

Evaluation of Structural Nonlinearities Using the Method of Harmonic Balance[5]

The measured force-deflection diagram with hysteresis (Figure 5) which needs to be represented in the analysis, defines the force necessary to overcome the static friction, the effective backlash and the nearly frictionless deformation at large force amplitudes. Figure 6 illustrates, in principle, the linear approximation of hysteresis type deflection curves which would be accomplished for different amplitudes. Assuming sinusoidal motions, the moment of force can be transformed into a periodic representation. The first harmonic is used to describe the equivalent linear stiffness coefficient $C(\beta)$, and damping loss angle $\gamma(\beta)$ where

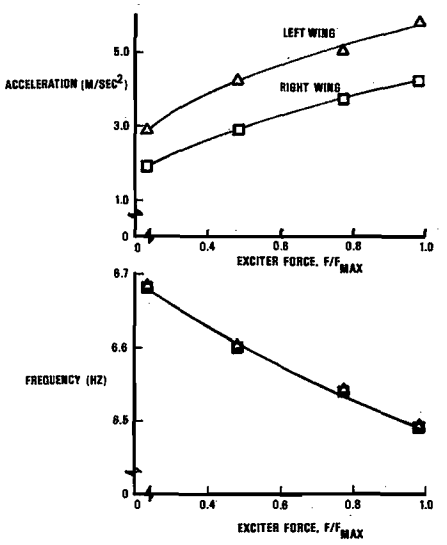

Figure 3. Ground Vibration Results for Store Pitch Mode

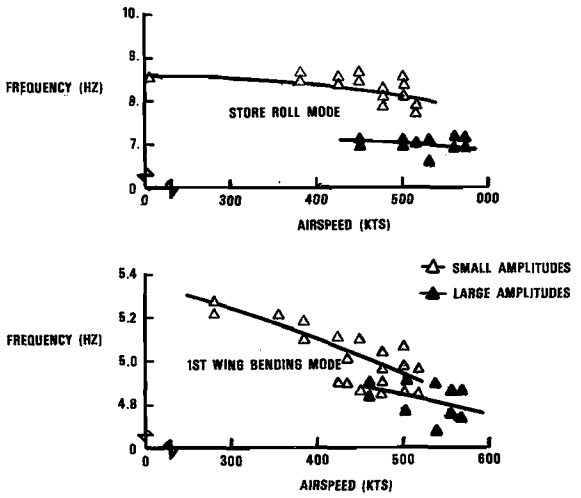

Figure 4. Frequency Variations in Flight Due to Structural Nonlinearities

$$C(\beta) = \frac{1}{\pi\beta} \int_{\zeta=0}^{2\pi} F(\beta \cos \zeta, -\beta\omega \sin \zeta) \cos \zeta d\zeta \quad (1)$$

$$\gamma(\beta) = \frac{1}{\pi\beta C(\beta)} \int_{\zeta=0}^{2\pi} F(\beta \cos \zeta, -\beta\omega \sin \zeta) \sin \zeta d\zeta \quad (2)$$

These values can then be introduced into conventional calculations to predict nonlinear flutter.

Control Law Definition

The best control law is one which provides the required stability (including phase and gain margins) with the least motion of the control surface due to external disturbances. Such a law can be theoretically found by applying optimal

control theory[6]. Equation (3) shows the state space description of the equation of motion for the forced dynamic response of the aeroelastic system.

$$\{\dot{x}\} = [A]\ \{x\} + \{B\}\ \{x_i\}. \qquad (3)$$

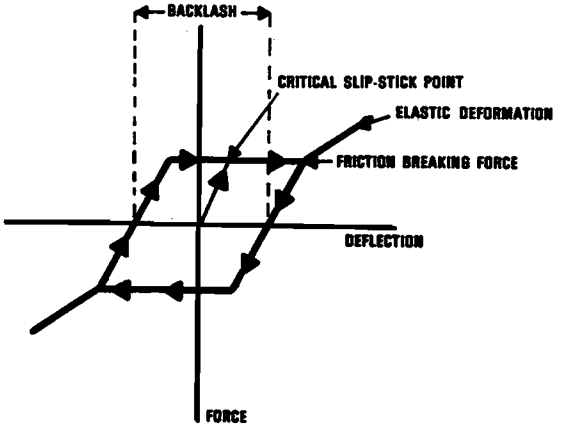

Figure 5. Hysteresis Diagram

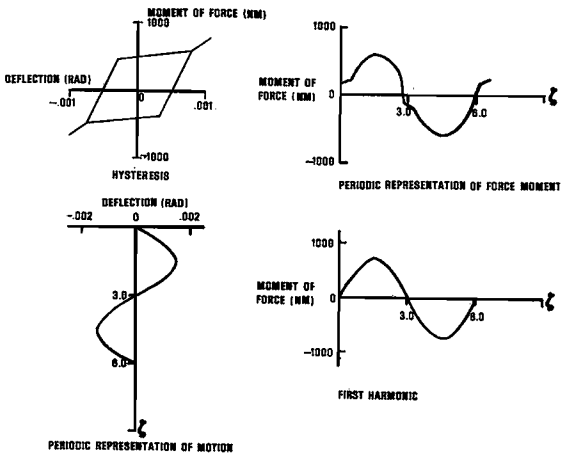

Figure 6. Linearization of Measured Deflection Curves by the Harmonic Balance Method

In this equation, {x} is defined as the state vector

$$\{x\} = \begin{Bmatrix} q \\ \beta_0 \\ \Delta\beta \\ \dot{q} \\ \dot{\beta}_0 \\ \Delta\dot{\beta} \end{Bmatrix} \qquad (4)$$

and $\{x_i\}$ is the actuator input signal. For the study reported herein, q represents the wing bending and store pitch modes, β_0 is the aileron elastic deflection, and $\Delta\beta$ is the aileron control deflection. The Matrices [A] and {B} consist of elements defined by the aeroelastic properties (mass, stiffness, damping and reference parameters).

To obtain the optimal control law $\{k_{opt}\}$ the quadratic performance criterion

$$J = \int_0^\infty (\{x\}^T\ [Q]\ \{x\} + x_i R\ x_i)dt \qquad (5)$$

is minimized. [Q] is defined as a weighting matrix found by trial and error, and R is a scalar (to be selected) since there is only one control surface. Minimizing J leads to the optimal control law

$$x_i = \{K_{opt}\}^T\ \{x\} \qquad (6)$$

with

$$\{K_{opt}\}^T = -R\ \{B\}^T\ [P] \qquad (7)$$

where [P] is the steady state solution of the Matrix Riccati equation

$$[-\dot{P}] = [P][A]+[A]^T[P]-[P]\{B\}\ R^{-1}\{B\}^T[P]+[Q]. \qquad (8)$$

Because there is no direct access to the state vector {x}, linear combinations of the sensor outputs can be used to obtain the state terms

$$\{y\} = [C]\ \{x\} \qquad (9)$$

where {y} is the sensor output, and [C] is a transformation matrix. Figure 7 shows the block diagram for this model. The control vector $\{K_m\}$ which is related to the measured vector {y} can be defined by the inverse transformation matrix $[C^{-1}]$ by

$$\{K_m\}^T = \{K_{opt}\}^T\ [C^{-1}] \qquad (10)$$

For the final design of the control law, it was found that the contribution of the states related the aileron elastic deflection (β_0) was small, and therefore, no feedback of those state was necessary.

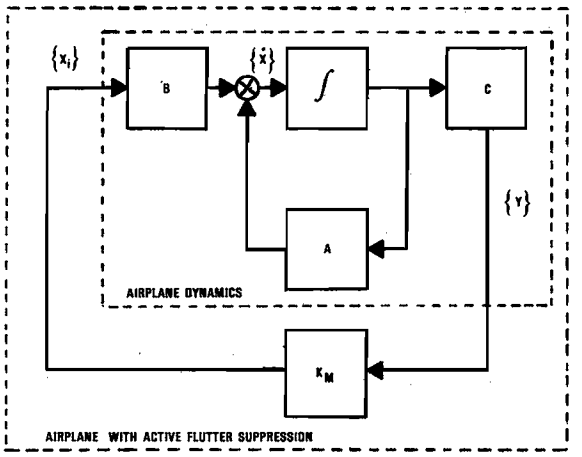

Figure 7. Block Diagram of the Airplane with Active Flutter Suppression

To perform the system-on flutter calculations, an approximated transfer function of the active flutter suppression system was introduced into the mathematical model. These transfer functions

are based on measured data from the full scale hardware. Figure 8 shows the transfer function of the complete aileron actuating system with a modified high-gain National Waterlift Power Actuator. The transfer function of the control electronics with a bandpass filter included to avoid detrimental coupling of the active flutter suppression system with rigid body modes is shown in Figure 9. The unsteady aerodynamic forces were calculated using both the doublet lattice method[7] and the lifting surface method by Laschka[8]. Figure 10 shows the damping versus velocity with the control law operating. For zero damping an improvement of almost 300 kts in flutter speed was predicted with the system on.

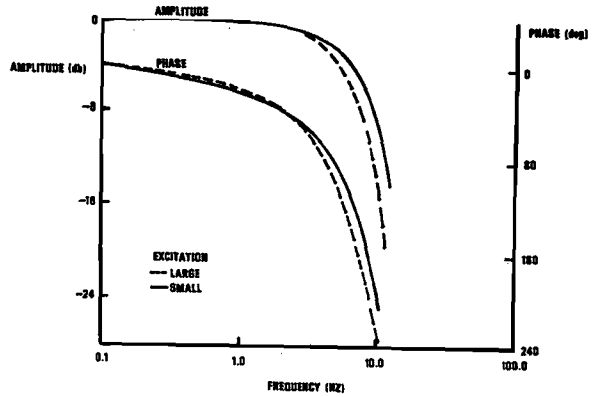

Figure 8. Transfer Function of the Aileron Actuating System

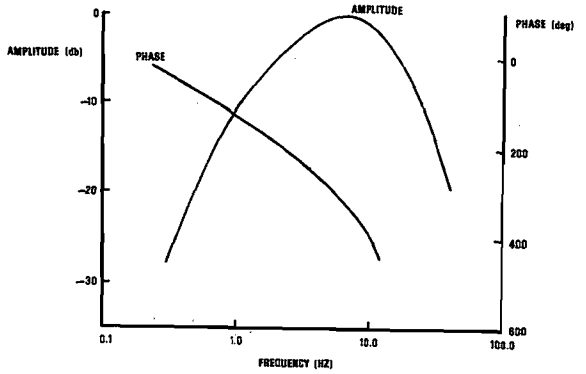

Figure 9. Transfer Function of the Control Electronics

Implementation and Safety Requirements

Because the aircraft was already equipped for store flight flutter testing, only minor modifications were necessary for the implementation of the system. Figure 11 presents a schematic of the airplane, showing the location of the feedback sensors, the active ailerons, the flight test equipment, and the active flutter suppression control box and panels that were installed. For the store configuration selected for the F-4 test, flutter could be described by two modes: the first wing bending and the first wing torsion/store pitch mode. These modes could be measured by three accelerometers on the wing. The output of the flutter suppression

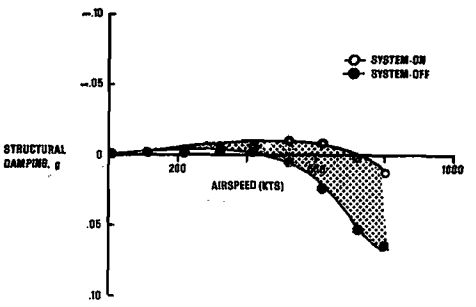

Figure 10. Calculated Damping Versus Velocity for the F-4F with Active Flutter Suppression

control box was fed into the roll channel of the stability augmentation system. To avoid mechanical coupling with the spoilers, the ailerons were biased downward by 2.5°. For safety of flight, two active flutter suppression systems (one on each wing) working independently were implemented. Either one was able to suppress flutter up to a certain speed. If both systems failed, an automatic electrical system which responds to a preselected wing amplitude would activate the mechanical flutter stopper. This signal would release the trim weights in the store in about 0.5 seconds, creating a flutter-safe radius of gyration. Both stores are designed with flutter stoppers, and either one would be able to suppress flutter by creating an asymmetric store combination. If necessary, the stores could be jettisoned by the pilot to increase flutter safety.

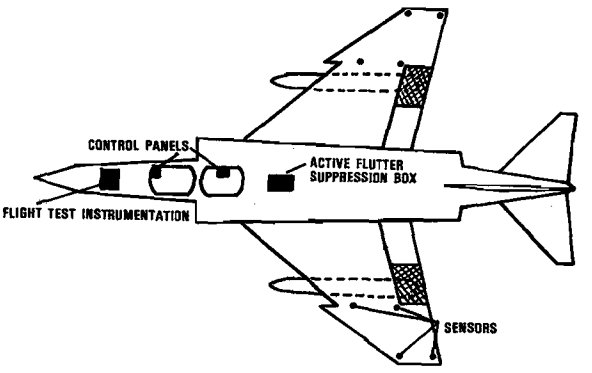

Figure 11. Schematic of System Implementation

Ground and Flight Test Activities

An extensive structural mode coupling test was performed to check out the system with the inertia forces present, and to determine the presence of adverse coupling of the system with higher frequency elastic modes. Nyquist plots were measured and compared with calculated data for zero airspeed. Good correlation was obtained.

The flight test program was divided into three major tasks. The first task represented the classical flight flutter tests to define the flutter speed boundary for both the flutter-critical and flutter-safe store configurations. The second task involved open loop tests to verify or tune the analytically defined control law. The last test which has not yet been accomplished, provides proof of concept and will involve an evaluation of the system performance at high speeds.

Figures 12 and 13 present damping trends for the wing bending and store pitch modes with the system off for both the flutter-critical and flutter-safe configurations. The airplane was excited with a frequency sweep input into the ailerons. The damping and frequency of the two modes were found by using the Hewlett Packard 5451 B computer and special MBB software. Figure 12 shows passive flutter to occur at about 600 kts while Figure 13 shows that the flutter-safe configuration has about 4% structural damping at 600 kts.

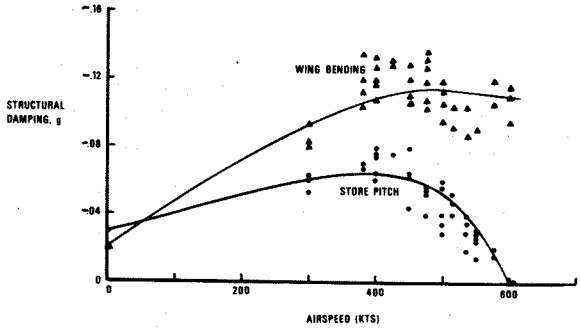

Figure 12. Measured Damping Trend for the Critical Store Configuration

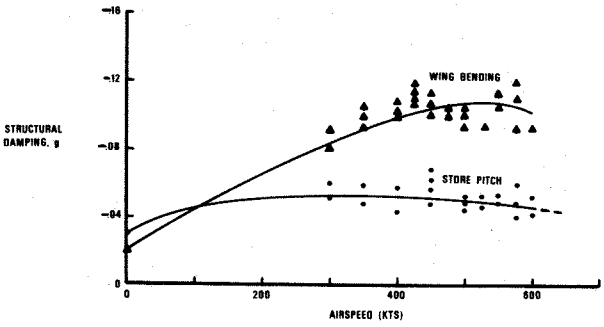

Figure 13. Measured Damping Trend for the Flutter-Safe Store Configuration

Open loop test results are shown in Figure 14 for different sensor locations at approximately the same airspeed. It was determined that Combination I and II could not be used because the outer wing bending mode at 11.3 Hz could become unstable with the right conditions. Combination III provided the best response; however, a counterclockwise phase shift is necessary for the pitch mode (5.5 Hz) to be optimally suppressed. This phase shift was due to the actuator transfer function which has more phase lag than the one which was used in the calculation to develop the control law. Such open loop tests are necessary because the system with state vector feedback takes into account only two modes (store pitch and first wing bending), and all other modes must be excluded by bandpass compensation or filtering by sensor location.

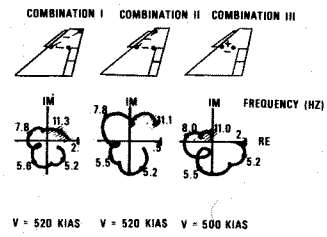

Figure 14. Effect of Sensor Locations on Nyquist Diagrams

Limited closed loop tests were performed at subcritical speeds to demonstrate elastic mode suppression. Tests have shown that when the right system was exciting and the left was damping, vibration amplitudes at 5 Hz were reduced considerably on the left wing. A higher frequency mode at 8 Hz remained unchanged because the active flutter suppression system was not designed to be effective in that range.

High speed and supercritical tests (tests above the passive flutter speed) have not yet been accomplished. Plans are to demonstrate the active flutter suppression system in the fall of 1980. Based on the results obtained to date, the system should perform as predicted.

AFWAL YF-17 WIND TUNNEL TEST PROGRAM

Through the auspices of USAF data exchange agreements with several European organizations, the French (Office National d'Etudes et de Recherches Aerospatiales), the British (Royal Aircraft Establishment and British Aerospace) and the Germans (Messerschmitt-Bolkow-Blohm) were invited to participate in the YF-17 active flutter suppression wind tunnel test program. Through a NASA grant with Israel, the Technion Israeli Institute of Technology was also invited to participate. Each organization developed control laws which were mechanized and implemented by the Northrop Corporation. These laws were developed for a specific flight condition ($M = 0.8$) and for a single store configuration (AIM-7S on an outboard underwing pylon). The design goal was to obtain a 30% improvement in the flutter speed while maintaining gain margins of ±6 db and phase margins of ±60°. The tests were conducted with the cooperation of the NASA LaRC in the 16-foot TDT during October 1979.

In support of these tests, AFWAL performed analyses to provide predictions for correlation with the available test data. Although the design and tests were conducted at $M = 0.8$, analyses were also performed at several Mach numbers covering the range from $M = 0.6$ to $M = 0.95$ to determine system effectiveness at the off-design conditions.

This section provides a description of the wind tunnel model, and a discussion of the MBB control law design, test results and predicted

performance at off-design conditions.

AFWAL YF-17 Active Flutter Suppression Model

The flutter model shown in Figure 15 represents an advanced lightweight fighter wing (YF-17). To simulate the symmetric flutter characteristics, the semispan flexible wing and fuselage model was designed to be wall mounted with rigid-body pitch and plunge degrees of freedom. Both leading and trailing edge control surfaces (independently actuated by electro-hydraulic devices) were used either singly or in combination for active flutter suppression. Four accelerometers located in the outer wing were used to measure the model response. The feedback signal could involve any combination of the four sensors or could include a blending of displacements, velocities and accelerations. A schematic of the model showing the planform dimensions, and control surfaces and sensor locations is provided in Figure 16.

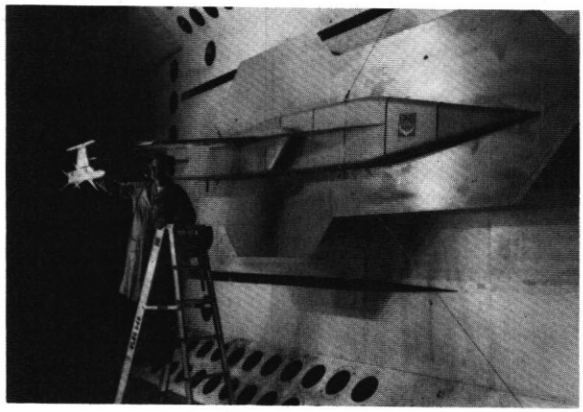

Figure 15. Wind Tunnel Model with AIM-7S Missile

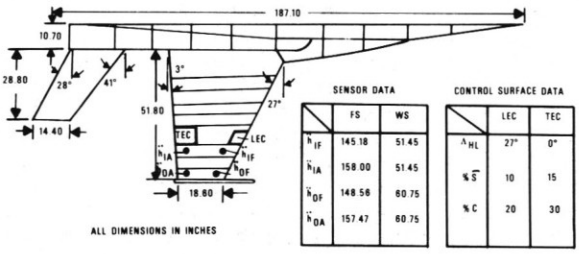

Figure 16. Wind Tunnel Model Planform Dimensions

The store configuration selected for the test was an AIM-7S missile mounted on an outboard wing pylon and an empty tip launcher rail (Figure 15). This configuration was selected because of the clearly defined flutter condition obtained in previous tunnel tests. Also, the violent nature of flutter for this configuration presented a challenging case for evaluating the effectiveness of a store flutter suppression system.

Similar to the F-4 project, the wind tunnel model was equipped with a flutter detector and stopper to protect the model in case of unexpected flutter occurrences or other instabilities. The flutter detector was used to define when a flutter condition or other divergent oscillation existed. It consisted of an electronic circuit which determined when the amplitude of signals from the model were above a preset level and when a certain number of consecutive pulses exceeded the preset level. When these two conditions were met, a signal was generated to activate the flutter stopper. The flutter stopper involved the AIM-7S with an internal spring-loaded movable mass. In case of flutter, the mass would be released by a solenoid mechanism and would travel about 25 cm in approximately 1/4 second. Once the movable mass was in the safe position, it could be reset from a remote site (control room) to any desired location for further testing.

MBB Control Law Design[9]

For the design analyses conducted by MBB, the unsteady aerodynamic forces were calculated using the first eight measured vibration modes of the model (rigid body modes of pitch and plunge were neglected). To obtain the unsteady aerodynamic forces, it was assumed that the aerodynamic forces of the tailplane had no influence on the wing flutter mechanism, and that the lift due to the missile body and the missile-wing interference were negligible. The unsteady wing aerodynamic forces were calculated at M = 0.8 using the doublet lattice method[7] and the lifting surface method by Laschka[8]. Because theory in general overpredicts control surface aerodynamics, the trailing edge forces were multiplied by a factor of 0.7 prior to designing the control law.

Optimal control theory, similar to the procedure discussed earlier, was used by MBB to design the active flutter suppression system. For this design, the trailing edge surface was selected as the force producer. The control law was found by using only two generalized coordinates (wing bending and wing torsion) since the flutter mode was a pure binary. A bandpass filter was used to decouple the system from the rigid body and high frequency elastic modes. Figure 17 shows the block diagram of the control law developed by MBB. Two inboard sensors were used to obtain torsional acceleration ($\ddot{h}_{IF} - \ddot{h}_{IA}$), and with the use of an inboard and an outboard sensor, acceleration related to bending ($\ddot{h}_{OF} - \ddot{h}_{IF}$) was obtained. These two signals were blended by four optimal coefficients (K_{ϕ}, $K_{\dot{\phi}}$, K_{θ}, and $K_{\dot{\theta}}$), and compensated by the bandpass filter. The Nyquist diagram and a V-g plot with the control law operating are shown in Figures 18 and 19 respectively. The dashed curve in Figure 19 represents the passive flutter results.

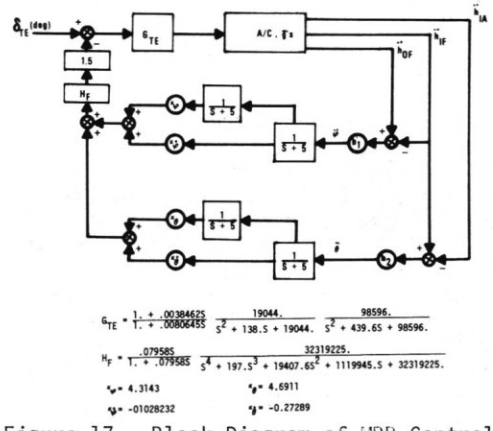

Figure 17. Block Diagram of MBB Control Law

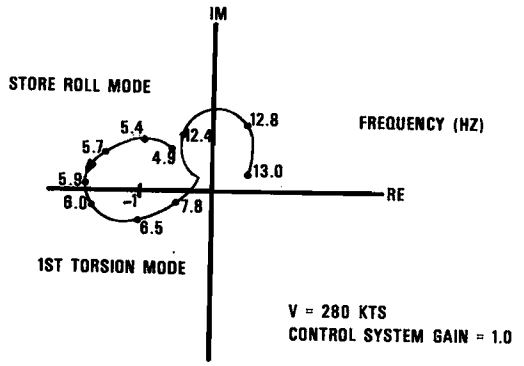

Figure 18. Nyquist Diagram of Control Law

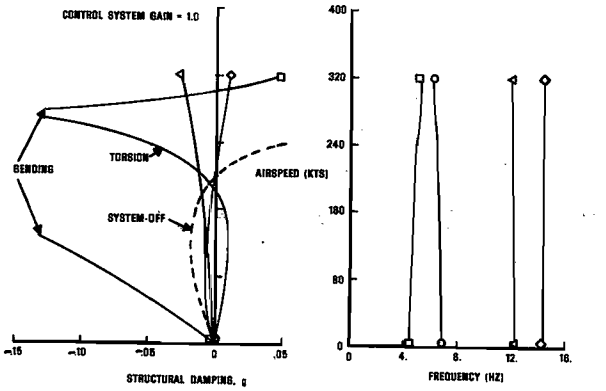

Figure 19. Damping and Frequency Versus Velocity with Control Law Operating

Wind Tunnel Test Results

The wind tunnel tests were conducted in October 1979 in the NASA Langley 16-foot TDT. All testing was accomplished at a M = 0.8 flight condition. The peak-hold spectrum method was used throughout the tests to provide a measurement of the model response for varying test condition or control law parametric changes. The peak response, filtered through 250 narrow-band circuits, was registered on a screen until the peak amplitudes ceased to grow. An indication of the damping of each resonant mode was obtained by taking the inverse of the peak amplitude at that mode frequency. Damping trend data could be extrapolated as the dynamic pressure was increased to determine the projected flutter dynamic pressure for either a controlled or uncontrolled system. Typical examples of this method are plotted in Figure 20. The inverse of the amplitude for the bending peak of Figure 20 is plotted in Figure 21 versus airspeed. The model would flutter at the speed where this value becomes zero. Figure 20 indicates the same behavior as shown in the V-g plot of Figure 19; the torsion mode is suppressed with increasing speed, and the bending mode is approaching an instability.

Figure 22 shows the model flutter speed versus total gain of the active flutter suppression system. From this figure it can be deduced that an increase in gain above 0.7 increased the flutter speed very little and would only make the system sensitive to disturbances. The phase

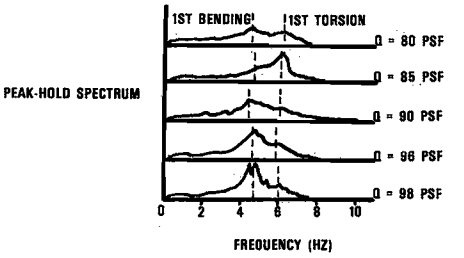

Figure 20. Peak-Hold Diagrams for Various Speeds M = 0.8, Control System Gain = 1.0

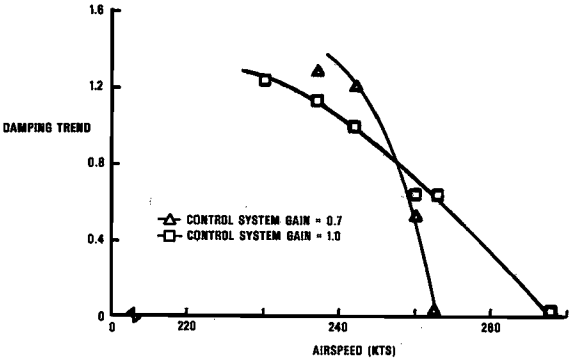

Figure 21. Inverse Amplitude Versus Speed

margins of ±60° could not be fulfilled with this control law, however, the ±6 db gain margin could almost be met. Figure 23 shows good correlation of test results with analytical predictions. Test data was projected to show a 22% increase in the flutter speed when the system was operating.

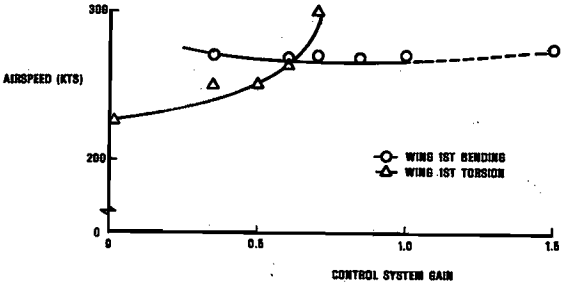

Figure 22. Flutter Speed Versus Gain

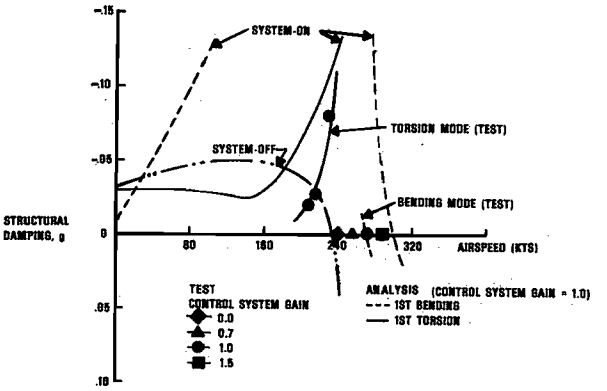

Figure 23. Comparison of Test Results and Predictions

After an evaluation of wind tunnel test results, two major deficiencies in the design were found. It was determined that the bandpass filter used had large phase shifts in the range from 4 Hz to 8 Hz (about 90° phase lag), and that it was not included in the optimization procedure but just compensated for at one distinct frequency. A new bandpass filter was designed which had almost the same attenuation behaviour as the one used in the test, but with much less phase shift in the range 4 Hz to 8 Hz (about 20° phase lag). Having calculated a new control vector, a Nyquist diagram was made at a speed of 280 knots. This diagram (Figure 24) now shows a perfect circle which infers superior phase margins over the initial control law.

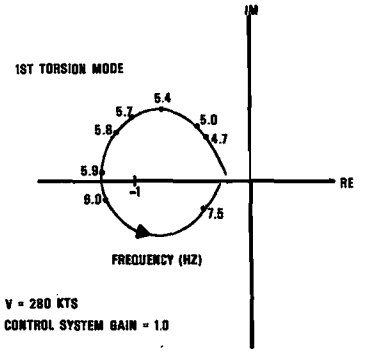

Figure 24. Nyquist Diagram of Improved Control Law

Control at Off-Design Flight Conditions[10]

Analyses were performed by AFWAL to evaluate the off-design characteristics of the MBB control law at Mach numbers varying from 0.6 to 0.95. For these analyses, the calculated trailing edge unsteady aerodynamics were used unmodified (they were not reduced by a factor). The passive and system-on instabilities obtained from the projected test data are also included in the figures for correlation.

The flutter dynamic pressure (Figure 25) was predicted by analysis to decrease from 153 psf to 112 psf as the Mach number was increased from M = 0.6 to 0.9. At a Mach number greater than 0.9, the instability was predicted to change to the higher frequency fuselage first-bending mode. This caused a more rapid drop in flutter dynamic pressure to about 80 psf at M = 0.95 which is 14% lower in dynamic pressure than the system-off condition. At the test condition of M = 0.8, the system-on flutter dynamic pressure was calculated to be 18% higher than the projected test point. The improvement in flutter dynamic pressure over the passive results with the active system on was 48% based on test data, and 60% based on analysis.

To add more insight into the change in critical mode near M = 0.95, the calculated system-on damping curves for both the bending mode and the fuselage bending mode are presented in Figure 26. The curves show that the damping in the fuselage bending mode decreases with increasing Mach number until the model becomes unstable. Because of the very low damping values predicted for the mode, the inclusion of structural damping in the analysis would eliminate this changing of critical modes. Figures 27 and 28 present the gain and phase margin plots, respectively, for this control law.

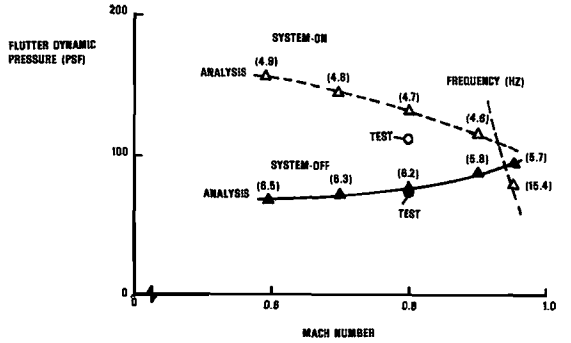

Figure 25. Mach Number Effects on Flutter

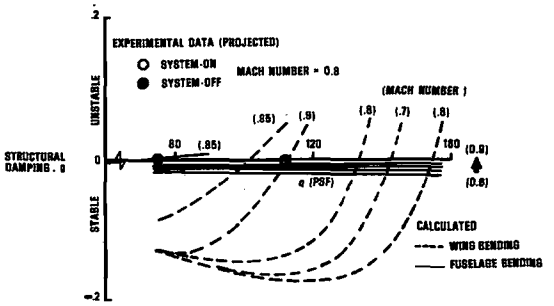

Figure 26. Calculated Damping with Control Law Operating

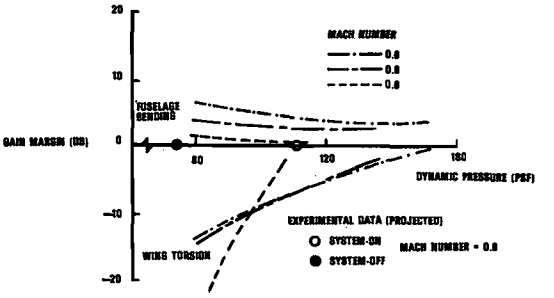

Figure 27. Calculated Gain Margins with Mach Number

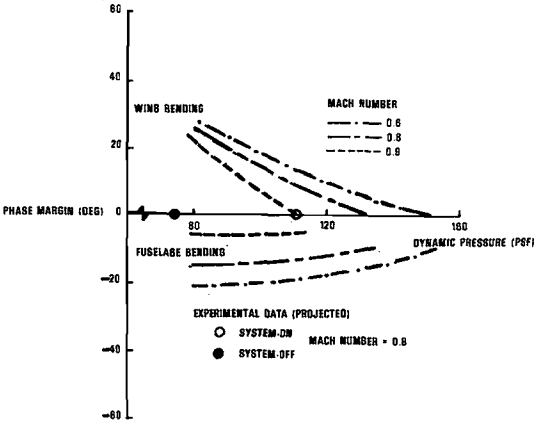

Figure 28. Calculated Phase Margins with Mach Number

Based on these and other calculations on several control laws[10], variations in Mach number were shown to have a significant effect on control law performance. Besides a reduction in flutter dynamic pressure, variations in Mach number have been shown to cause changes in the mode of instability. In some cases, control system-induced instabilities in either low or high frequency modes were predicted. For this model, increasing Mach number added phase lead to the system, while increasing dynamic pressure provided either phase lead or phase lag depending on the control law. For those cases where a change in the mode of instability was predicted to occur, it was attributed to a combination of these two effects (lag resulted in higher frequency mode instabilities while lead resulted in lower frequency instabilities). These analyses indicate that the active flutter suppression design approach must take into consideration the operation of the law over the entire flight envelope. This could be accomplished by some form of optimal law that performs satisfactorily at all conditions, or through adaptive principles.

Conclusions

In the last five years, active control of wing/store flutter has been of significant interest both within the United States and in Europe. The state of the art in this technology has been extended from simplified feasibility calculations through complex wind tunnel and flight investigations. Through a cooperative international research effort between the United States and Germany, a wing/store active flutter suppression system has been successfully designed, fabricated and implemented on an F-4F aircraft. Although the final high speed flights have not yet been accomplished, open loop tests indicate that the system will perform as expected. This program also identified the seriousness of structural and control system nonlinearities on the flutter characteristics of the aircraft.

Through a separate AFWAL wind tunnel test program, the talents of many organizations were integrated to develop, test and evaluate active control laws for a single severe flutter condition on a common wind tunnel model. Using various design approaches, each of the control laws succeeded in preventing flutter to very respectable limits. The control law developed by MBB was one of the more challenging ventures in that the trailing edge surface was selected for control. This difficult task was due to the position of the surface and the fixed sensors which were required to be used.

The background and technical data base is now available for a detailed flight test demonstration of the concept. This investigation should fully evaluate features such as system compatibility with the airframe and flight control, operation during severe maneuvers and turbulence, fail safe requirements and redundancy, advances in fly-by-wire and digital flight control technology, and other operational considerations. However, taking into account the basic nature of wing/store flutter, additional development is still required in the area of adaptive control. Within the near future and following successful completion of the above programs, the technology will be available for integration into advanced aircraft designs or for retrofitting derivatives of existing aircraft.

References

1. Sensburg, O., Hönlinger, H., Noll, T. E., "Active Flutter Suppression on a F-4F Aircraft with External Stores Using Already Existing Control Surfaces", Paper presented at the 21st Structures, Structural Dynamics and Materials Conference of the AIAA, 12-14 May 1980, Seattle/Washington, U.S.A.

2. Hwang, C., Winther, B. A., Noll, T. E., Farmer, M. G., "Demonstration of Aircraft Wing/Store Flutter Suppression Systems", AGARD Report No. 668, Paper presented at the 46th SMP of AGARD, 10-14 April 1978, Aalborg/Denmark.

3. Hwang, C., Johnson, E. H., Mills, G. R., Noll, T. E., Farmer, M. G., "Wind Tunnel Test of a Fighter Aircraft Wing/Store Flutter Suppression System - An International Effort", Paper presented at the 50th Meeting of the SMP of AGARD, 13-18 April 1980, Athens/Greece.

4. Triplett, W. E., Landy, R. J., Irwin, D. W., "Preliminary Design of Active Wing Store Flutter Suppression Systems for Military Aircraft", AFFDL-TR-74-67, August 1974.

5. De Ferrari, G.,Chesta, L.,Sensburg, O., Lotze, A., "Effects of Nonlinearities on Wing Store Flutter", Paper presented at the 50th Meeting of the SMP of AGARD, 13-18 April 1980, Athens/Greece.

6. Sensburg, O., Zimmermann, H., "Impact of Active Control on Structures Design", Paper presented at teh AGARD Multi-Panel Symposium "Fighter Aircraft Design", 3-6 October 1977, Florence/Italy.

7. Giesing, J. G., Kalman, T. P., Rodden, W. P., "Subsonic Unsteady Aerodynamics for General Configurations", AIAA Paper 72-76, 1972.

8. Laschka, B., "Zur Theorie der harmonisch schwingenden tragenden Flache bei Unterschallstromung, ZFW, Heft 7, 1963.

9. Sensburg, O., Hönlinger, H., Schneeberger, B., Kuhn, M., "Review of Active Flutter Suppression Tests and Analyses on AFFDL Model of YF-17" paper presented at NASA LaRC, 8-9 May 1980.

10. Noll, T. E., Huttsell, L. J., Cooley, D. E., "Investigation of International Control Laws for Wing/Store Flutter Suppression", Paper presented at the AIAA 21st SDM Conference, Seattle/Washington, May 1980.